

# Brazilian Tests on Transversely Isotropic Rocks: Laboratory Testing and Numerical Simulations

Xin Tan · Heinz Konietzky · Thomas Frühwirt ·  
Dinh Quoc Dan

Received: 30 January 2014 / Accepted: 22 May 2014 / Published online: 5 July 2014  
© Springer-Verlag Wien 2014

**Abstract** The dominant anisotropy (foliation and bedding) of geological materials, especially of foliated metamorphic rocks such as slates, gneisses, phyllites or schists, and sedimentary rocks with bedding planes, leads to complex fracture mechanical behavior. A series of Brazilian tests on Mosel slate were conducted considering different foliation-loading angles. Fracture patterns and strength of samples were analyzed. In addition, the deformation process and failure behavior of the foliated rock samples during the Brazilian tests were simulated using the discrete element method. The influence of anisotropic strength parameters of weak planes was studied numerically. A diagram of failure mode distribution marked with typical failure fracture patterns for Brazilian tests of transverse isotropic rocks was developed, which results in better understanding of failure modes of Brazilian tests on foliated rocks and allows a more reliable interpretation of strength parameters. It reveals, how the microparameters influence the bearing capacity and failure modes of Brazilian tests for anisotropic rocks.

**Keywords** Brazilian test · Anisotropy · Transversely isotropic rock · Discrete element method · Numerical simulation · Fracture pattern

## 1 Introduction

The mechanical behavior of rocks is often influenced by the fabric structure, i.e., bedding, stratification, layering, foliation, fissuring or jointing; in other words, by anisotropy. Anisotropy can be found at different scales. It affects the stability of geotechnical structures and has influence on geotechnical operations like drilling, blasting, and rock cutting (Chen et al. 1998). Therefore, there is a strong need for better understanding the anisotropic properties and their adequate application in geotechnical design (Tavallali and Vervoort 2010). Many researchers (e.g., Istvan et al. 1997; McLamore and Gray 1967; Seto et al. 1997) have studied the tensile strength of anisotropic rocks using the Brazilian test. The effect of layer orientation on strength and fracture pattern of sandstone (Chen et al. 1998; Tavallali et al. 2007, 2008), transversely isotropic artificial rocks (Tien et al. 2006) and layered slate (Debecker and Vervoort 2009) has been studied. A comprehensive analytical solution for an anisotropic disc subjected to compressive load was presented by Amadei et al. (1983), based on a solution method developed by Lekhnitskii (1968). Chen et al. (1998) presented a combination of analytical and experimental methods for determination of elastic constants and Brazilian tensile strength of transversely isotropic rocks.

This study presents a numerical approach to study in detail the fracture patterns of transversely isotropic rocks using data of layered slate tested via the Brazilian method. Fracture pattern and strength of samples under different foliation-loading angles were analyzed. The influence of foliation-loading angle was studied through experiments and numerical simulations. This combined approach gives a better understanding of failure modes and allows a more reliable interpretation of strength values.

---

X. Tan  
College of Civil Engineering, Geotechnical Institute, Hunan  
University, Changsha, Hunan, China

H. Konietzky (✉) · T. Frühwirt · D. Q. Dan  
Geotechnical Institute, TU Bergakademie Freiberg,  
Gustav-Zeuner-Str. 1, 09599 Freiberg, Germany  
e-mail: heinz.konietzky@ifgt.tu-freiberg.de

## 2 Experimental Procedure

### 2.1 Sample Preparation and Test Apparatus

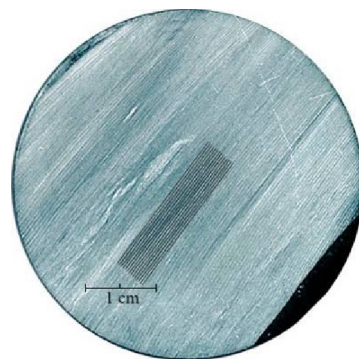
The highly transverse isotropic Mosel slate (My.Sc) from Mayen-Koblenz in Rheinland-Pfalz (Germany) was chosen for this study. The slate has dense parallel planes of weakness with one dominant direction. The layers have a thickness of  $<0.5$  mm (Fig. 1a).

The recommendations of the International Society for Rock Mechanics (ISRM 1978) and the German Geotechnical Society (Deutsche Gesellschaft für Geotechnik 2008) were followed strictly during sample preparation and testing. The specimens are disc-shaped with a diameter  $D = 50$  mm and a thickness  $t = 25$  mm. First, cylindrical cores with a diameter of 50 mm were drilled out of larger rock blocks. It was especially ensured that the axis of the cylindrical cores was parallel to the strike of the foliation planes. The cores were then cut into test specimens of suitable length. The end faces were ground. If the dimensions of the specimens were found to meet the standards, the specimens were stored in dry air at room temperature (Dan et al. 2013). The uniaxial rock mechanical test system MTS 20/M (loading capacity of 100 kN) was used for the Brazilian tests.

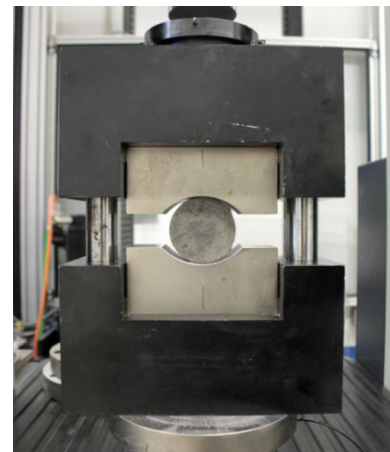
### 2.2 Experimental Method and Results

The experimental arrangement for the Brazilian tests is illustrated in Fig. 1b and c, with special emphasis on orientation of layering. The planes of layering are planes of weakness, characterized by significant reduced cohesive and tensile strength. The foliation-loading angle ( $\theta$ ) is the angle between the loading direction and the layering. By changing  $\theta$  in steps of  $15^\circ$ , seven different constellations were tested. The disc was loaded with a constant loading rate of 200 N/s until failure. Four samples were tested for each  $\theta$ -value. The strength was calculated according to the analytical solution developed by Hondros (1959). The calculated “tensile strength” values of each sample are listed in Table 1. Typical fracture pattern are shown in Figs. 2 and 6. The “tensile strength” here means the maximum tensile stress at the center of disc sample when the sample lost its total bearing capacity. The term “tensile strength” is set into quotation marks, because pure tensile fracturing is observed only for special configurations depending on the foliation-loading angle. Within this article, independent on the observed fracture pattern, all evaluations are performed according to the classical equation for Brazilian tests, which assumes isotropic homogeneous material:

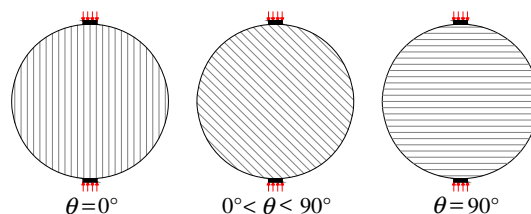
**Fig. 1** Experimental arrangements for testing rock anisotropy



(a) My.Sc slate sample.



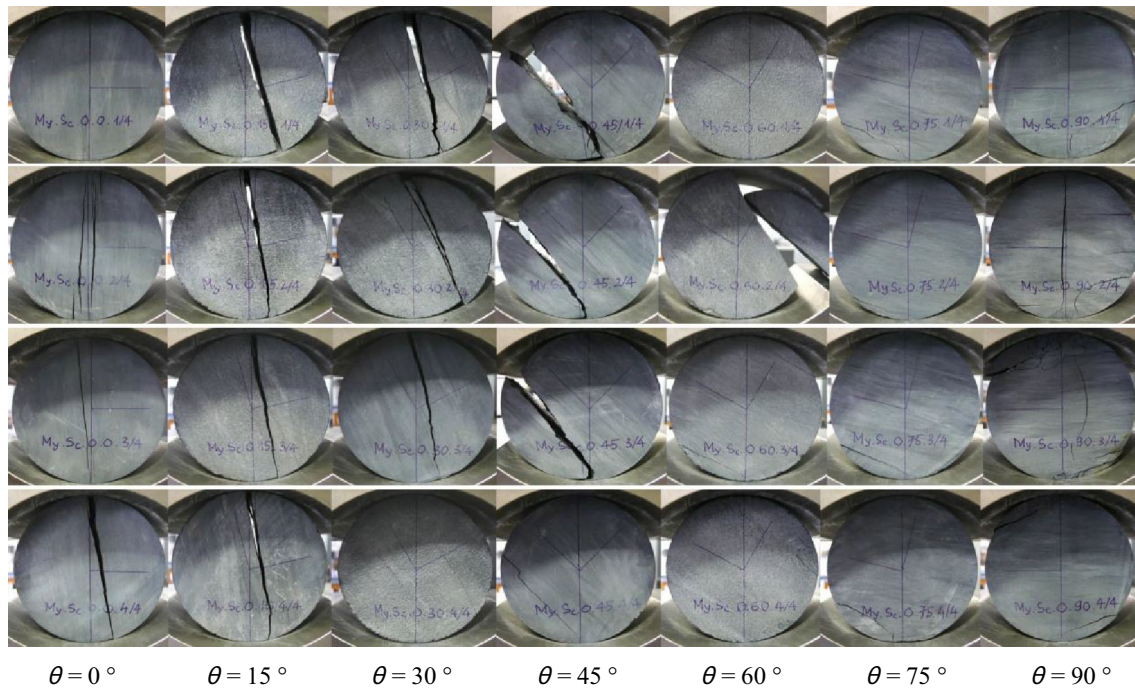
(b) Brazilian test set-up with sample and loading jaws.



(c) foliation-loading angle  $\theta$

**Table 1** “Tensile strength” of the Mosel slate samples (MPa)

$\theta$	0°	15°	30°	45°	60°	75°	90°
My.Sc. 1/4	2.385	2.595	2.375	3.39	3.389	8.106	14.878
My.Sc. 2/4	3.143	3.225	3.67	5.631	3.67	8.925	15.013
My.Sc. 3/4	5.353	4.581	4.579	5.972	3.846	9.419	15.312
My.Sc. 4/4	5.985	4.782	4.975	6.582	7.811	10.189	17.022
Mean	4.22 ± 1.8	3.80 ± 1.2	3.90 ± 1.5	5.39 ± 2.0	4.68 ± 3.1	9.16 ± 1.1	15.56 ± 1.5
SD	1.72	1.06	1.15	1.39	2.1	0.87	0.99
Coef. Var	41 %	28 %	30 %	26 %	45 %	10 %	6 %

**Fig. 2** Fracture patterns of Mosel slate discs under different foliation-loading angles

$$\sigma_T = 2P/\pi D, \quad (1)$$

where  $\sigma_T$  is the “tensile strength”,  $P$  is the peak loading force,  $l$  the length, and  $D$  the diameter of the disc-shaped sample.

It is observed that the “tensile strength” is maximal (about 15–16 MPa) when the loading direction is orthogonal to the foliation ( $\theta = 90^\circ$ ) and decreases rapidly with decrease in  $\theta$ . The “tensile strength” becomes minimal and remains nearly constant (about 4–6 MPa) for  $\theta$  smaller than  $60^\circ$ . The laboratory tests show, that the orientation of the layered structure in relation to the loading direction has a strong influence on the measured peak strength obtained from Brazilian tests and that fracture patterns as shown in Fig. 2 are strongly influenced by the rock structure.

### 3 Numerical Simulation Using Discrete Element Modeling

#### 3.1 The Discrete Element Method

The existence of pronounced discontinuities in rocks (cracks, joints, bedding, foliation, etc.) limits the applicability of continuum based numerical methods to solve rock mechanical problems. Therefore, various discontinuum mechanical approaches have been developed to address this topic. Nowadays, the discrete element method (DEM) is the most popular among them (Jing and Hudson 2002). The key concept of DEM is to treat the domain of interest as an assemblage of rigid and/or deformable blocks/particles and to identify and continuously update the contacts among the blocks during the entire deformation/motion

process. Appropriate constitutive models are applied at the contacts. The most popular DEM computer code for solving two-dimensional problems in rock mechanics is UDEC (Cundall and Hart 1992; Itasca 2006).

In UDEC, a rock or rock mass is represented as an assembly of discrete blocks (polyhedra). Joints are considered as interfaces between these distinct bodies. The contact forces and displacements at these interfaces of a stressed assembly of blocks are found through a series of calculations that trace the movements of the blocks. The dynamic behavior is represented numerically by a time-stepping algorithm in which the size of the time step is limited by the assumption that velocities and accelerations are constant within the time step.

### 3.2 Simulation Procedure

The rock is represented by deformable blocks, which are cemented to each other along their contacts. The layering (weak planes) is represented by joints with lower strength. A numerical slate sample is shown in Fig. 3. The parallel joints have a spacing of 0.3 mm.

The detailed model setup is shown in Fig. 3b, where Zone 1 and Zone 2 represent the loading jaws and the rock specimen, respectively. The model consists of elastic blocks and several sets of joints with different stiffness

values. Joint 1 is active only inside the loading jaws. Joint 2 is the interface between the loading jaws and the rock sample. Joint 3 represents the rock matrix and Joint 4 the weak planes (layering).

The deformability of meshed blocks is governed by bulk and shear modulus,  $K$  and  $G$ . The deformability of joints is described by normal and shear stiffnesses,  $k_n$  and  $k_s$ . The strength of joints is described by friction angle  $\phi^j$ , cohesion  $c^j$ , and tensile strength  $\sigma_t^j$ . In this numerical model, disc sample deformability is controlled by both the stiffness parameters of zones and joints, while strength is controlled by strength parameters of joints only. The postpeak behavior of joints is perfectly brittle. Once the tensile strength or shear strength is reached, the joint loses its virgin strength (tensile strength and cohesion are set to zero), and the normal displacement during shearing is controlled by the dilatancy angle  $\psi^j$ .

Deformability and strength parameters of slate are listed in Table 2. Unlike continuum models, the input parameters (such as stiffness and strength) cannot be derived directly from laboratory measurements. The tensile strength  $\sigma_t^j$  of

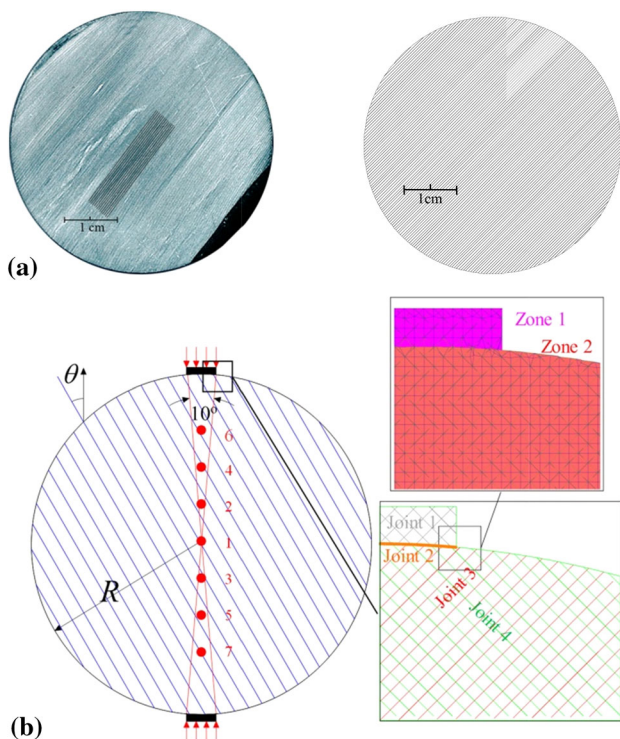


**Fig. 3** a Slate disc model (left: photograph of laboratory sample, right: numerical model); b numerical model setup

**Table 2** Summary of mechanical parameters (Barton 1976; Goodman 1989; Hoek 2007, and own results)

Mechanical parameters	Literature records	Laboratory results	UDEC Input	UDEC Output
Young's modulus $E$ (GPa)	35.0–47.0	45.0		45.2
Poisson's ratio $\nu$	0.3–0.45	0.33		0.33
Bulk modulus $K$ (GPa)			150 (Zone 2)	
Shear modulus $G$ (GPa)			60 (Zone 2)	
Normal stiffness $k_n$ matrix (Pa/m)			$2.70 \times 10^{14}$ (Joint 3)	
Shear stiffness $k_s$ matrix (Pa/m)			$1.05 \times 10^{14}$ (Joint 3)	
Normal stiffness $k_n$ joint (Pa/m)			$2.10 \times 10^{14}$ (Joint 4)	
Shear stiffness $k_s$ joint (Pa/m)			$7.20 \times 10^{13}$ (Joint 4)	
Tensile strength $\sigma_t^m$ matrix (MPa)		15.5	15.0 (Joint 3)	15.2
Tensile strength $\sigma_t^j$ joint (MPa)		4.2	5.0 (Joint 4)	4.4
Cohesion $c^m$ matrix (MPa)	10.3–32.0		32.0 (Joint 3)	
Cohesion $c^j$ joint (MPa)	5.0–13.2		10.0 (Joint 4)	
Friction $\phi^m$ matrix ( $^\circ$ )	43.7–50.0		50 (Joint 3)	
Friction $\phi^j$ joint ( $^\circ$ )	22.6–44.4		40 (Joint 4)	

Joint 3 and Joint 4 is set equal to the tensile strength valid for the foliation-loading angles of  $\theta = 90^\circ$  and  $\theta = 0^\circ$ , respectively, which indicates either pure tensile failure in

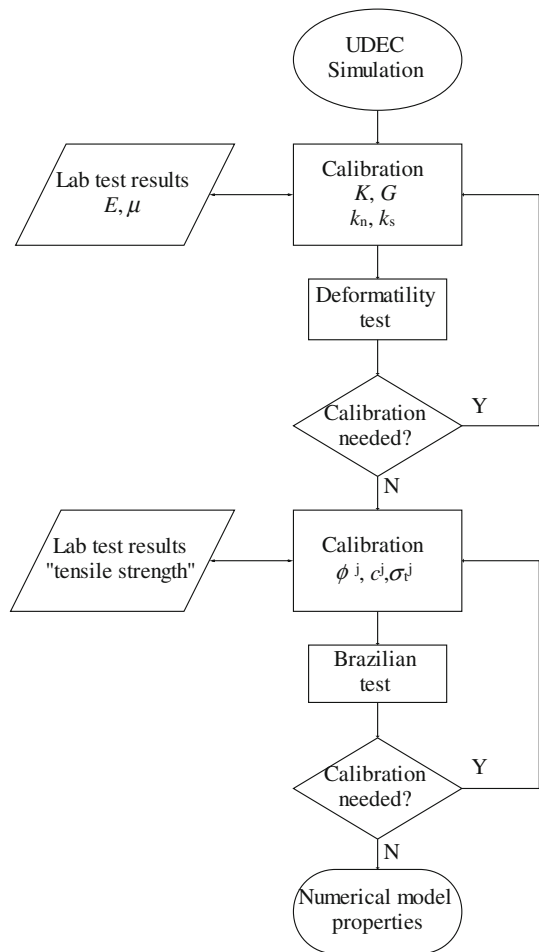


Fig. 4 Model parameter calibration procedure

rock matrix or weak planes (Table 1). The shear strength parameters (friction and cohesion) were first derived from the literature (Table 2) and later adjusted in such a way, that they match the measured “tensile strength” for different foliation-loading angles. A calibration procedure illustrated in Fig. 4 was used to determine micromechanical parameters, which match the macroscopic behavior and parameters, respectively. The final parameters obtained from calibration and subsequently used for the simulations are shown in Table 2.

To simulate the Brazilian tests, load is applied through loading jaws by applying a constant velocity at both top jaws and bottom jaws. The force between the loading jaws and the disc is transmitted via a frictionless interface, which has a central angle of  $10^\circ$  (Fig. 3b). The parameters of loading jaws (Zone 1 and Joint 1) and interface (Joint 2) have significantly higher values compared to rock material in order to simulate a nearly rigid and indestructible material. Seven points as marked in Fig. 3b were chosen to trace the tensile stress variations during the loading process along the vertical central line of the disc.

#### 4 Comparison Between Experiment and Simulation

##### 4.1 “Tensile Strength”: Comparison Between Laboratory Results and Numerical Simulations

Simulation results for different  $\theta$  are presented in Fig. 5. Special attention was paid to the stress component perpendicular to the vertical disc axis at the center of the sample (point 1 in Fig. 3b), since the classical evaluation is based on the assumption that it is the center where the

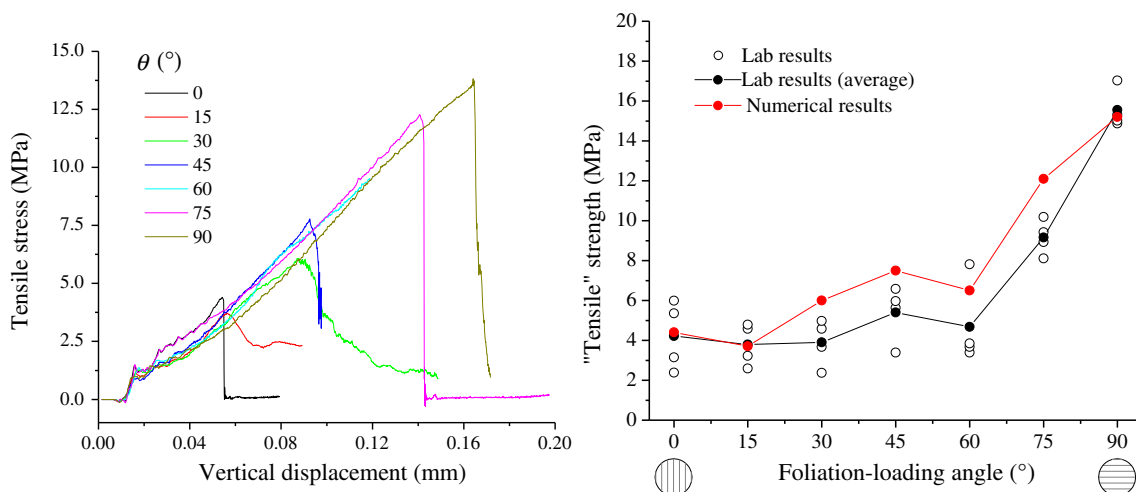
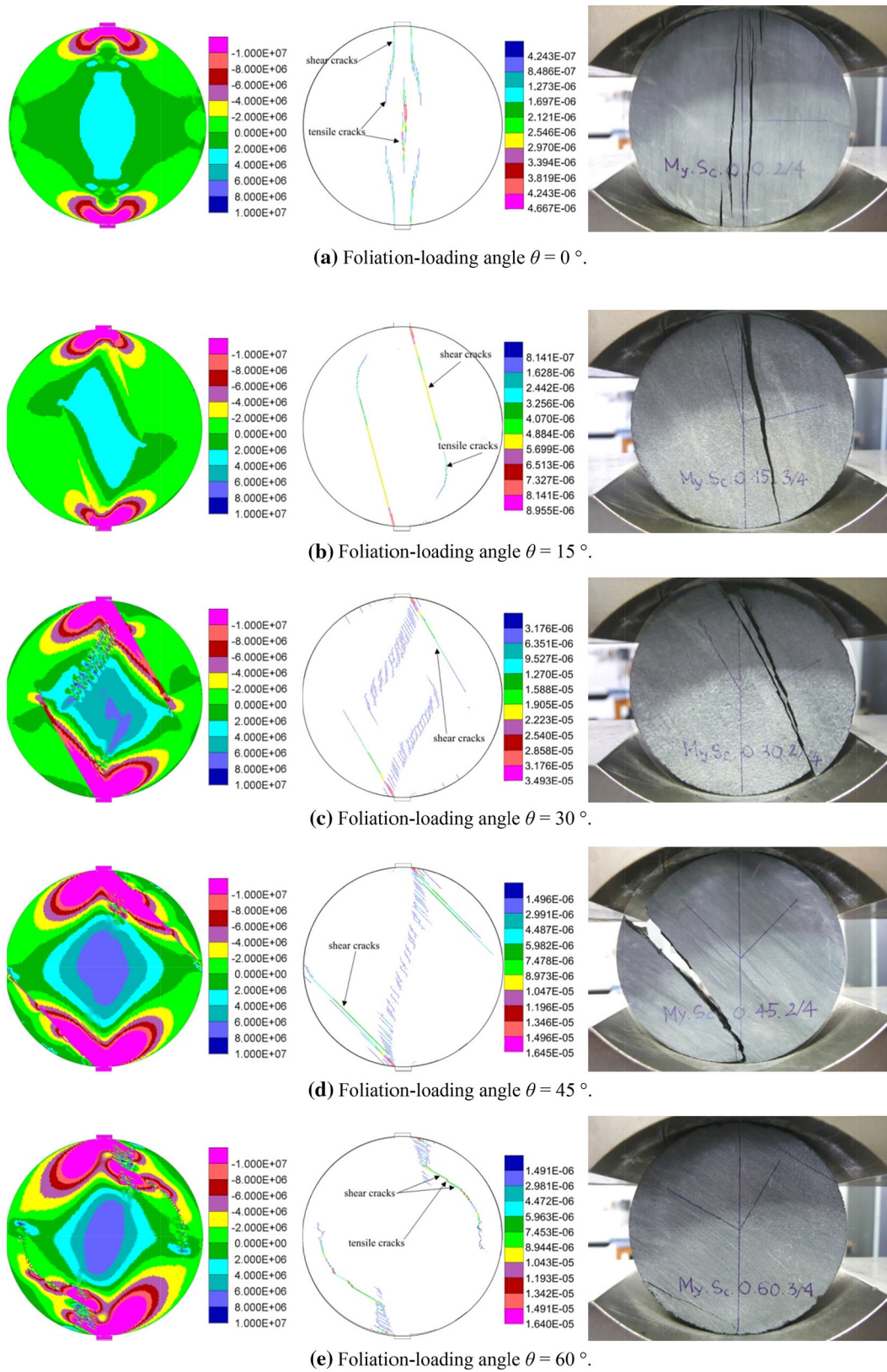


Fig. 5 a Horizontal stress (tensile stress) at the center of sample (point 1) vs. vertical displacement; b “Tensile strength” of numerical models in comparison with laboratory results



**Fig. 6** Fracture patterns for different foliation-loading angles for Mosel slate. (Left tensile stress distribution (Pa); middle fracture opening (m); right fracture pattern observed in laboratory)

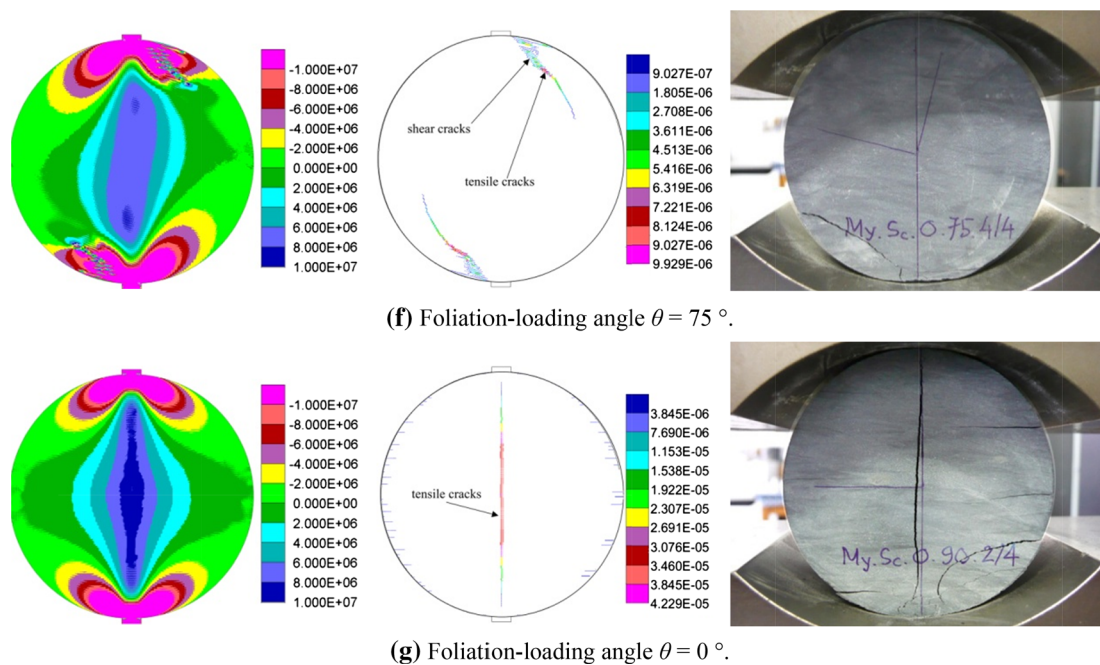


Fig. 6 continued

maximum tensile stress occurs and where the tensile cracking is initiated.

The prepeak behavior of the models with different  $\theta$  is quite similar. However, the maximum tensile stress and the corresponding displacements increase with increasing  $\theta$ . Figure 5b documents a comparison between laboratory test results and the numerical simulations, which shows a good agreement. This indicates that the measured peak “tensile strength” is very sensitive to the foliation-loading angle.

#### 4.2 Fracture Pattern: Comparison Between Laboratory Results and Numerical Simulations

Figure 6 shows a typical fracture pattern of My.Sc slate observed in the laboratory and during numerical simulations.

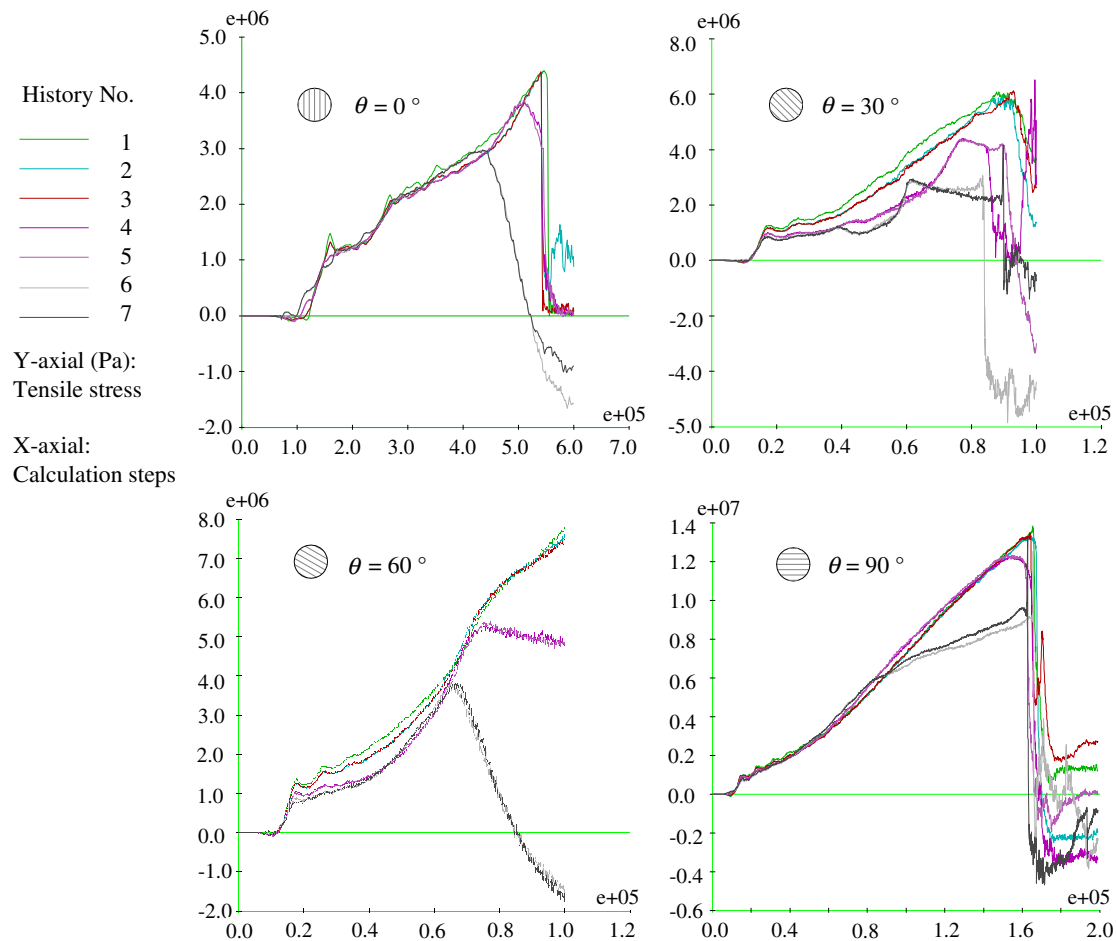
The fracture pattern at  $\theta = 0^\circ$  is very similar to the isotropic case. Cracks initiate at the center of the disc, grow further in direction towards the loading jaws, and finally penetrate the whole sample. However, the peak tensile stress is 4.4 MPa, which is much lower than the tensile strength of the rock matrix. This indicates that tensile cracks develop along the schistosity planes (tensile stresses exceed the tensile strength of these planes). Also, some shear cracks develop near the loading jaws after the formation of the main central tensile fracture.

Figure 6b, c and d ( $\theta = 15^\circ, 30^\circ$  and  $45^\circ$ ) show typical shear fractures along the schistosity planes. Cracks initiate at the contacts between rock and loading jaws where shear

stress concentrates. Finally, a main shear fracture penetrates the whole sample along the direction of the schistosity planes. The main fracture does not cross the center of the disc and no tensile cracks are formed at the center of the disc. Compared to the intact rock material, the schistosity planes have a quite low shear strength. Therefore, shear failure takes place before the tensile strength of the intact material is reached, which means that the measured peak strength is not related to the tensile strength. The measured peak stress increases with increasing  $\theta$ , because the effect of the increasing normal stresses on the schistosity planes exceeds that of increasing shear stresses.

Figure 6e, f ( $\theta = 60^\circ$  and  $75^\circ$ ) show a more complex fracture pattern. With increase in  $\theta$ , resistance against shear failure along schistosity planes increases. Shear cracks initiate at the contact between rock and the loading jaws, but they do not develop any longer as single straight fractures. Several tensile cracks are initiated in the rock matrix because of increasing load level and the relative movement between schistosity planes. These tensile cracks influence the development of the main fracture. Therefore, some curved macrofractures appear. This mixed mode failure type is characterized by combined tensile splitting and shear failure. Fracturing takes place along the schistosity planes as well as in the rock matrix.

The fracture pattern at  $\theta = 90^\circ$  is similar to that at  $\theta = 0^\circ$ . Cracks initiate at the center of the disc and propagate towards the loading jaws until they penetrate the sample completely. The peak tensile stress is 15.2 MPa,



**Fig. 7** Numerical tensile stress variations for marked points during the loading process

which is much higher than the tensile strength at  $\theta = 0^\circ$ . The main failure mechanism in this case is tensile splitting of the rock matrix, and the corresponding tensile strength can be deduced.

Zhou et al. (2014) recorded the crack growth process by using a high-speed camera in dynamic Brazilian tests of granite. The initial crack propagated from the disc center to the boundary, which shows similar crack growth process compare to numerical results of  $\theta = 0^\circ$  and  $90^\circ$ .

Development of the tensile stresses for several observation points according to Fig. 3 is shown in Fig. 7. Pronounced differences can be observed for different failure types and foliation-loading angles. For pure tensile failure ( $\theta = 0^\circ$  and  $90^\circ$ ) the main tensile fracture develops across the center of the disc; therefore, the tensile strength is lost in observation points along the vertical central line once the peak tensile stress is reached at central point (No. 1). For shear failure or mixed mode failure ( $\theta = 30^\circ$  and  $60^\circ$ ), the main fracture does not cross the center of the disc. Therefore, a progressive decrease but no ad hoc full reduction of tensile stress at the points along the vertical

center line is observed. Tensile stress of some points even increase continuously after the formation of the macrofracture as shown for  $\theta = 60^\circ$  in Fig. 7.

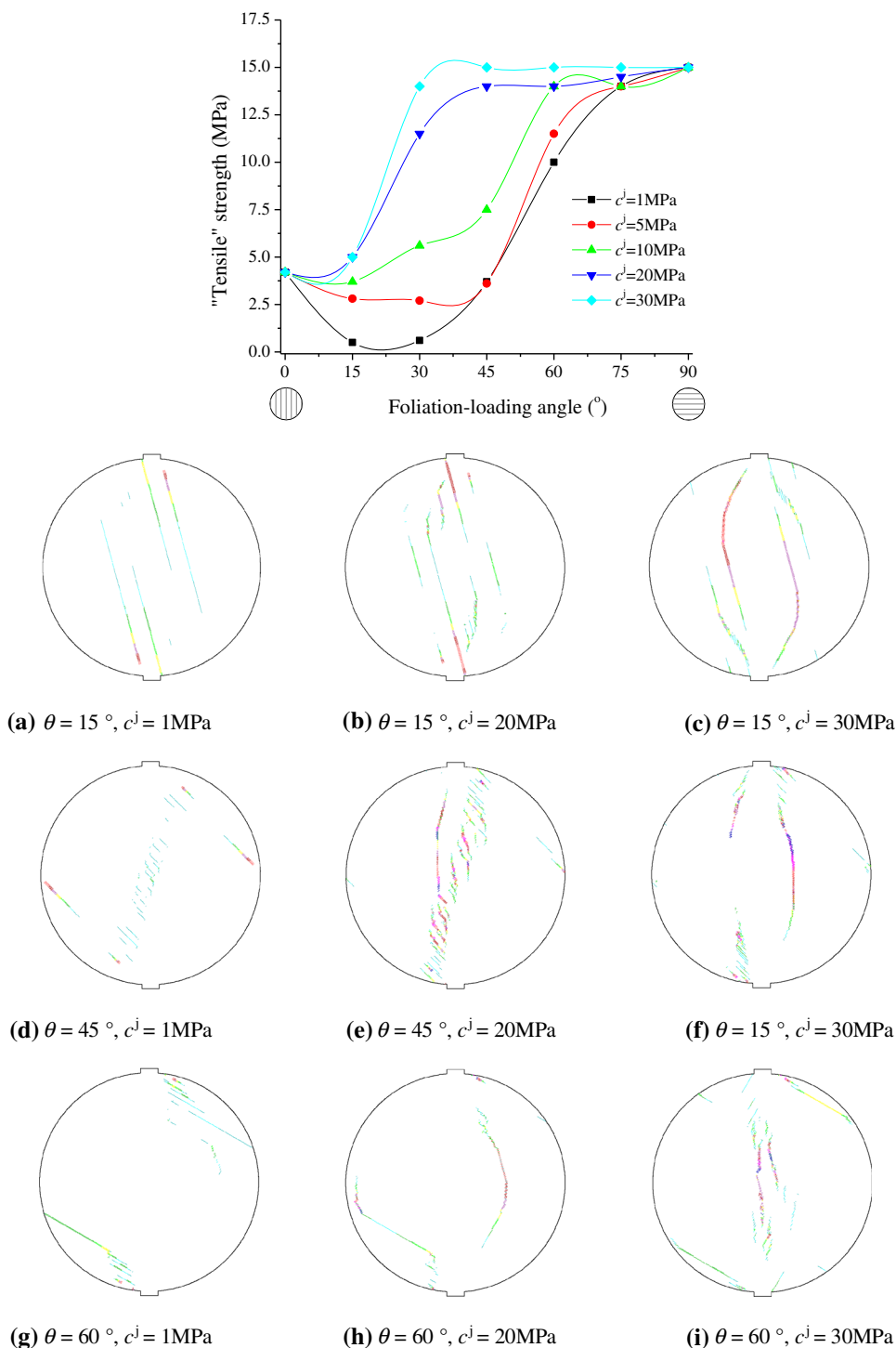
## 5 Influence of Joint Shear Strength

In order to investigate the influence of schistosity plane (joint) shear strength on failure behavior during the Brazilian test, a series of numerical simulations were conducted with different cohesion values  $c^j$  (1, 5, 10, 20 and 30 MPa). All other parameters were kept constant. The maximum tensile stresses at the center of the samples are shown in Fig. 8. The corresponding fracture patterns are shown in Fig. 8a–i.

Under constant foliation-loading angle  $\theta$ , the maximum tensile stress increases with increasing cohesion  $c^j$ . Under the condition of constant cohesion  $c^j$ : when  $c^j$  is low, the maximum tensile stress first decreases with increasing  $\theta$ , then increases until  $\theta$  exceeds a certain value, and finally approaches the tensile strength of the rock matrix; when  $c^j$



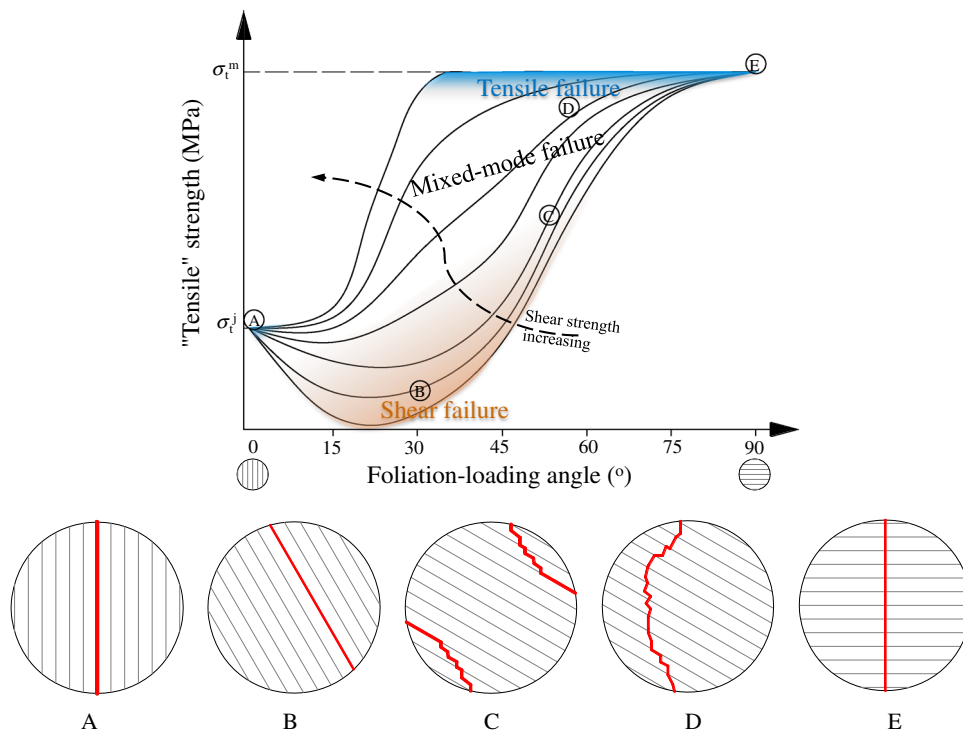
**Fig. 8** Maximum tensile stress at the center of numerical models and fracture patterns observed in numerical simulations



is high, the maximum tensile stress increases monotonously with increasing  $\theta$  and finally approaches the tensile strength of the rock matrix. It is worth remarking in general that the maximum tensile stress at the center of the sample cannot be considered as tensile strength, because in most cases the sample fails due to mixed-mode failure and the final macroscopic fracture does not cross the center of the disc.

As shown in Fig. 8a, d and g, the samples fail due to pure shear failure along the schistosity planes with very low cohesion  $c^j$  and finally shear fractures penetrate the whole disc along the direction of foliation. With increasing cohesion  $c^j$ , some tensile cracks develop within the rock matrix, which finally lead to a mixed-mode failure pattern (Fig. 8b, c, e, h). The mixed-mode failure pattern can be subdivided: Fig. 8b and c show mixed-mode failure pattern

**Fig. 9** Schematic representation of typical failure modes in Brazilian tests: *A* pure tensile failure along foliation; *B* pure shear failure along foliation; *C* mixed-mode failure in foliation and rock matrix (primary caused by shear failure); *D* mixed-mode failure in foliation and rock matrix (primary caused by tensile failure); *E* pure tensile failure across rock matrix



dominated by shear failure; and Fig. 8e and h show mixed-mode failure pattern governed by tensile failure. When the cohesion  $c^j$  comes close to the cohesion of the rock matrix, the sample exhibits tensile failure. The macroscopic fractures are curved because of layer interfaces (Fig. 8f, h, i).

Based on the evaluation of the abovementioned numerical simulations, a diagram of failure mode distribution for Brazilian tests of transversely isotropic rocks was developed (Fig. 9). It shows that pure tensile failure appears only in narrow regions around  $\theta = 0^\circ$  and  $90^\circ$  as well as for higher values of  $\theta$  in case of high shear strength along planes of anisotropy meaning that shear strength of foliation becomes nearly equal to that of the rock matrix. Five typical failure modes are marked in the diagram. Mixed-mode failure is common in Brazilian tests of transversely isotropic rocks, which should be taken into account for any kind of evaluation. Again, it should be considered, that the classical evaluation according to formulae 1 is based on the assumption of central tensile splitting, which is valid only for certain constellations. Therefore, the evaluation according to formulae 1 should be done with caution.

## 6 Conclusions

Brazilian tests performed on Mosel Slate show that the failure strength and the fracture pattern are considerably affected by the orientation of schistosity planes (foliation).

It is observed that the mean value of maximum tensile stress is 15.56 MPa when the loading direction is orthogonal to the foliation ( $\theta = 90^\circ$ ) and decreases rapidly with decrease of  $\theta$ , which indicates that the layer interface of the slate has much lower tensile and shear strength than the rock matrix. The Brazilian tests conducted on the slate were calculated back through numerical modeling based on the discrete element method. Pure tensile splitting was detected as failure mode for  $\theta = 0^\circ$  and  $90^\circ$ . There was a tensile failure for  $\theta = 0^\circ$  along schistosity planes and for  $\theta = 90^\circ$  in the rock matrix. When  $\theta$  gets larger ( $\theta = 15^\circ, 30^\circ$  and  $45^\circ$ ), the failure mode turns progressively into shear failure along schistosity planes, and the peak tensile stress increases with increasing  $\theta$ . Mixed-mode failure with tensile splitting and shear failure occurs at  $\theta = 60^\circ$  and  $75^\circ$ . Failure strength and fracture patterns obtained from numerical simulations are in good agreement with laboratory results. Therefore, the laboratory data and the calibrated microstrength parameters can be considered as potentially referential data for the future research and engineering community. Furthermore, the comparative investigation of the role of microparameter  $c^j$  and loading angle was conducted numerically, and a diagram of failure mode distribution marked with typical failure fracture patterns for Brazilian tests of transversely isotropic rocks was developed as shown in Fig. 9. Research results indicate that the material anisotropy has a significant influence on the stress distribution, crack initiation, fracture pattern, and bearing capacity. Mixed-mode failure is quite common

for Brazilian tests on transversely isotropic rocks. It also reveals how the bearing capacity and failure modes of Brazilian tests for transversely isotropic rocks are changed with foliation-loading angle, which results in a better understanding of failure modes of Brazilian tests on anisotropic rocks.

In order to simplify the numerical simulation scheme and to avoid potential complexity, some assumptions (frictionless interface, and central angle of  $10^\circ$ ) in relation to the interface between loading jaw and disc sample have been made. However, our own experience and knowledge based on a literature survey indicated that the loading conditions influence the fracture initiation of Brazilian tests. Further studies are necessary to investigate the role of loading conditions, which finally will allow us to draw more general conclusions.

## References

- Amadei B, Rogers JD, Goodman RE (1983) Elastic constants and tensile strength of the anisotropic rocks. Proceedings of the Fifth Congress of International Society of Rock Mechanics, Melbourne, pp 189–96
- Barton NR (1976) The shear strength of rock and rock joints. *Int J Mech Min Sci Geomech Abstr* 13(10):1–24
- Chen C, Pan E, Amadei B (1998) Determination of deformability and tensile strength of anisotropic rock using Brazilian tests. *Int J Rock Mech Min Sci* 35:43–61
- Cundall PA, Hart RD (1992) Numerical modeling of discontinue. In: Hudson JA (ed) *Comprehensive rock engineering*, vol 2, Oxford, pp 231–243
- Dan QD, Konietzky H, Herbst M (2013) Brazilian tensile strength tests on some anisotropic rocks. *Int J Rock Mech Min Sci* 58:1–7
- Debecker B, Vervoort A (2009) Experimental observation of fracture patterns in layered slate. *Int J Fract* 159:51–62
- Deutsche Gesellschaft für Geotechnik (2008) *Indirekter Zugversuch an Gesteinsproben—Spaltzugversuch*, Bautechnik, Ernst & Sohn, Berlin
- Goodman RE (1989) *Introduction to rock mechanics*. Wiley, New York
- Hoek E (2007) *Practical rock engineering*. <http://www.rocsience.com/hoek>. Accessed 22 Feb 2013
- Hondros G (1959) The evaluation of Poisson's ratio and the modulus of materials of a low tensile resistance by the Brazilian (indirect tensile) test with a particular reference to concrete. *Aust J Appl Sci* 10:243–268
- ISRM (1978) Suggested methods for determining tensile strength of rock materials. *Int J Rock Mech Min Sci* 15:99–103
- Istvan JA, Evans LJ, Weber JH (1997) Rock mechanics for gas storage in bedded salt caverns. *Int J Rock Mech Min Sci* 34:3–4
- Itasca (2006) *UDEC Universal Distinct Element Code—theory and background*. ICG, USA
- Jing J, Hudson JA (2002) Numerical methods in rock mechanics. *Int J Rock Mech Min Sci* 39:409–427
- Lekhnitskii SG (1968) *Anisotropic plates*. Gordon and Breach, New York
- McLamore R, Gray KE (1967) The mechanical behavior of the anisotropic sedimentary rocks. *J Eng Ind* 89:62–76
- Seto M, Nag DK, Vutukuri VS, Katasuyama K (1997) Effect of chemical additions on the strength of sandstone. *Int J Rock Mech Min Sci* 34:3–4
- Tavallali A, Vervoort A (2008) Failure of transversely isotropic rock material: effect of layer orientation and material properties. In: *Proceedings 6th International Symposium Ground Support, Mining, Civil Engineering and Construction*, Cape Town, pp 317–28
- Tavallali A, Vervoort A (2010) Effect of layer orientation on the failure of layered sandstone under Brazilian test conditions. *Int J Rock Mech Min Sci* 47:313–322
- Tavallali A, Debecker B, Vervoort A (2007) Evaluation of Brazilian tensile strength in transversely isotropic sandstone. In: Olalla C, Grossmann, Ribeiro L (eds) *Proceedings 11th International Congress Rock Mechanics*, Lisbon, pp 269–72
- Tien YM, Kuoa MC, Juang GH (2006) An experimental investigation of the failure mechanism of simulated transversely isotropic rocks. *Int J Rock Mech Min Sci* 43:1163–1181
- Zhou Z, Li X, Zou Y, Jiang Y, Li G (2014) Dynamic Brazilian tests of granite under coupled static and dynamic loads. *Rock Mech Rock Eng* 47:495–505